You might find this additional information useful...

This article cites 44 articles, 21 of which you can access free at:
http://jn.physiology.org/cgi/content/full/89/1/634#BIBL

This article has been cited by 32 other HighWire hosted articles, the first 5 are:

Distinct and Overlapping Functional Zones in the Cerebellum Defined by Resting State Functional Connectivity
J. X. O'Reilly, C. F. Beckmann, V. Tomassini, N. Ramnani and H. Johansen-Berg
Cereb Cortex, April 1, 2010; 20 (4): 953-965.
[Abstract] [Full Text] [PDF]

Cerebellar Engagement in an Action Observation Network
A. A. Sokolov, A. Gharabaghi, M. S. Tatagiba and M. Pavlova
Cereb Cortex, February 1, 2010; 20 (2): 486-491.
[Abstract] [Full Text] [PDF]

Cerebellar Inputs to Intraparietal Cortex Areas LIP and MIP: Functional Frameworks for Adaptive Control of Eye Movements, Reaching, and Arm/Eye/Head Movement Coordination
V. Prevosto, W. Graf and G. Ugolini
Cereb Cortex, January 1, 2010; 20 (1): 214-228.
[Abstract] [Full Text] [PDF]

Visual Motion Perception Deficits Due to Cerebellar Lesions Are Paralleled by Specific Changes in Cerebro-Cortical Activity
B. Handel, P. Thier and T. Haarmeier
J. Neurosci., December 2, 2009; 29 (48): 15126-15133.
[Abstract] [Full Text] [PDF]

Segregated Fronto-Cerebellar Circuits Revealed by Intrinsic Functional Connectivity
F. M. Krienen and R. L. Buckner
Cereb Cortex, October 1, 2009; 19 (10): 2485-2497.
[Abstract] [Full Text] [PDF]

Updated information and services including high-resolution figures, can be found at:
http://jn.physiology.org/cgi/content/full/89/1/634

Additional material and information about *Journal of Neurophysiology* can be found at:
http://www.the-aps.org/publications/jn

This information is current as of October 10, 2010 .

An Unfolded Map of the Cerebellar Dentate Nucleus and its Projections to the Cerebral Cortex

RICHARD P. DUM[2] AND PETER L. STRICK[1–3]
[1]*Pittsburgh Veterans Affairs Medical Center,* [2]*Center for the Neural Basis of Cognition, and Departments of Neurobiology,*
[3]*Psychiatry and Neurological Surgery, University of Pittsburgh School of Medicine, Pittsburgh, Pennsylvania 15261*

Dum, Richard P. and Peter L. Strick. An unfolded map of the cerebellar dentate nucleus and its projections to the cerebral cortex. *J Neurophysiol* 89: 634–639, 2003. First published November 6, 2002; 10.1152/jn.00626.2002. We have used retrograde transneuronal transport of neurotropic viruses to examine the organization of the projections from the dentate nucleus of the cerebellum to "motor" and "nonmotor" areas of the cerebral cortex. To perform this analysis we created an unfolded map of the dentate. Plotting the results from current and prior experiments on this unfolded map revealed important features about the topography of function in the dentate. We found that the projections to the primary motor and premotor areas of the cerebral cortex originated from dorsal portions of the dentate. In contrast, projections to prefrontal and posterior parietal areas of cortex originated from ventral portions of the dentate. Thus the dentate contains anatomically separate and functionally distinct motor and nonmotor domains.

INTRODUCTION

Traditionally, the dentate nucleus of the cerebellum was thought to project via the thalamus to a single cerebral cortical area, the primary motor cortex (M1) (e.g., Asanuma et al. 1983a; Kemp and Powell 1971; for references and review see Hoover and Strick 1999). According to this view, the output of the dentate was exclusively concerned with the control of movement. Recent studies have led to some significant alterations to this point of view. It is now clear that the dentate projection to M1 represents only a fraction of the output from the nucleus (Hoover and Strick 1999). Indeed, we have found that other portions of the dentate innervate oculomotor, prefrontal, and posterior parietal areas of the cerebral cortex (Clower et al. 2001; Lynch et al. 1994; Middleton and Strick 1994 2001). Furthermore, the projections to different cortical areas appear to originate from localized regions of the dentate, which we termed "output channels." This new anatomical data, along with results of behavioral and imaging studies (e.g., Fiez et al. 1992; Ivry et al. 1988; Jueptner et al. 1997; Kim et al. 1994; Mushiake and Strick 1993; Schmahmann 1997) have led to a reevaluation of dentate function (see Ramnani and Miall 2001; Special Issues of TINS 1998 and TICS 1998).

The complex morphology of the dentate imposes a major barrier for unraveling the functional organization of the nu-cleus. To overcome this problem, we developed an "unfolded" map of the nucleus. This map enables the dentate's intricate structure to be viewed as a flat surface (Fig. 1). In general, unfolded maps have considerable heuristic value in their capacity to reveal organizational features obscured by complex three-dimensional structure (Brodal 1940; Dum and Strick 1991; He et al. 1995; Larsell 1970; van Essen and Drury 1997; van Essen et al. 2001; van Essen and Maunsell 1980). Unfolded maps also provide a link between the neuroanatomy and physiology of the nonhuman primate brain and that of the human brain (van Essen and Drury 1997; van Essen et al. 2001). In the present study, we reanalyzed data from prior experiments at higher spatial resolution and replotted the results on our unfolded map of the dentate. These maps reveal a new perspective about the topographic organization of output channels within the dentate.

METHODS

Virus tracing

The results of this study are based on an analysis of data from experiments in which the McIntyre-B strain of herpes simplex virus type 1 (HSV1) was used as a retrograde transneuronal tracer to define the inputs to specific regions of motor, prefrontal, and posterior parietal cortex (Clower et al. 2001; Hoover and Strick 1999; Middleton and Strick 2001). The procedures adopted for this study and the care provided to experimental animals conformed to the regulations detailed in the *National Institutes of Health Guide for the Care and Use of Laboratory Animals*. All protocols were reviewed and approved by the Institutional Animal Care and Use committees. The biosafety precautions taken during these experiments conformed to or exceeded the Biosafety Level 2 regulations detailed in *Biosafety in Microbiological and Biomedical Laboratories* (Health and Human Services publication 93–8395). Detailed descriptions of the procedures for handling virus and virus-infected animals are presented in Strick and Card (1992) and Hoover and Strick (1999).

The details for these experiments have been described previously (Clower et al. 2001; Hoover and Strick 1999; Middleton and Strick 2001). Briefly, we injected virus into selected regions of the cerebral cortex of cebus monkeys (*Cebus apella*). The cortical regions injected were identified either by physiological mapping or by surface landmarks and their known relationship to the cytoar-

---
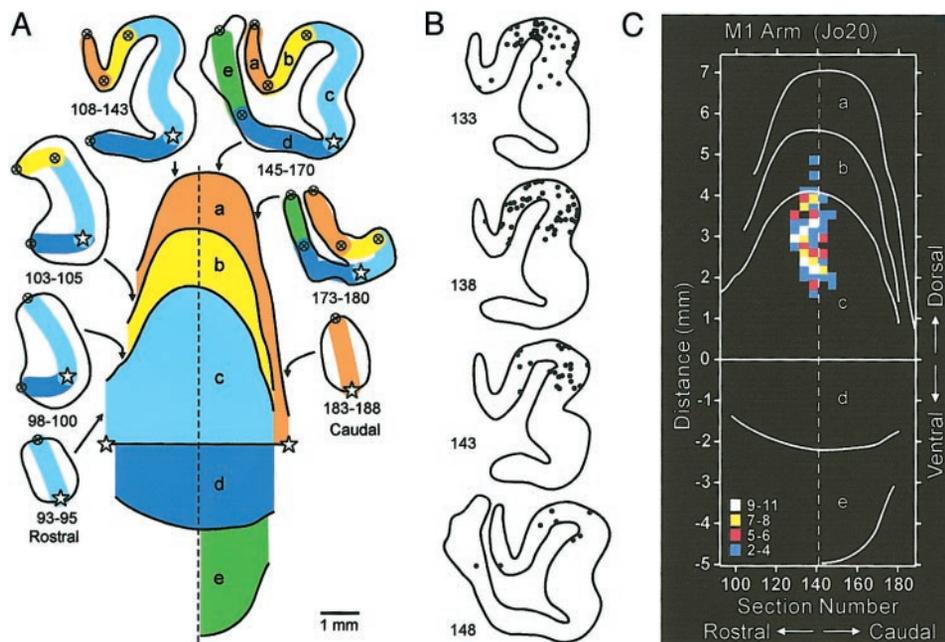
FIG. 1. Unfolded map of the dentate nucleus. *A*: this map of the dentate was created by unfolding serial coronal sections through the nucleus. Typical sections are displayed around the map to indicate the shape of the dentate at selected levels. The unfolding process began by drawing a line through the center of the nucleus on each section. The color-coded segments of these lines correspond to the colored regions on the unfolded map. Each section is aligned to the junction of the *c* and *d* segments (*open star*). The dashed vertical line indicates the rostrocaudal center of the nucleus. See Methods for further explanation. *B*: cross-sections of the dentate nucleus showing the location of "second order" neurons (*dots*) labeled after transport of herpes simplex virus type 1 (HSV1) from the arm representation of M1. *C*: distribution and density of labeled neurons in the same animal are displayed on an unfolded map of the dentate. This map was reconstructed from every other coronal section.

chitectonic borders of each cortical area. The locations of injections were later confirmed by cytoarchitectonic evaluation of the processed brain tissue. We used a postinjection survival time of 4–5 days. This survival time allows retrograde transport of HSV1 from the injection site to first-order neurons in the thalamus and then retrograde transneuronal transport from these first-order neurons to second-order neurons in the dentate nucleus. At the end of the survival period, each animal was deeply anesthetized and perfused with aldehyde fixatives. The cerebellum was frozen and serially sectioned (50 μm) in the coronal plane. To identify neurons infected with virus, we processed free-floating tissue sections according to the avidin–biotin peroxidase method (Vectastain, Vector Laboratories, Burlingame, CA) using a commercially available antibody to HSV1 (1:2,000 dilution, Dako, Carpinteria, CA).

Unfolded map

For the present study, we charted the outline of the dentate and the location of labeled neurons on every other serial section (for details, see Hoover and Strick 1999; Middleton and Strick 2001). Next, on each coronal section we drew a curved line through the nucleus midway between its medial and lateral outlines (Fig. 1*A*). The transitions between the major dentate segments and the position of each labeled neuron were projected onto the central line. Then, each line through the nucleus was unfolded and aligned on the transition between the "c" segment (the main vertical segment of the nucleus) and the "d" segment (the main ventral segment). This alignment minimizes the distortion of dentate regions that project to areas 4, 7b, 46, and 9l. To examine the density of labeled neurons we divided the unfolded lines into 200-μm intervals and totaled the number of labeled neurons in each interval. The values of intervals from adjacent lines were combined to form 200 $\times$ 200 μm bins. A color code was assigned to each bin to indicate the number of labeled neurons it contained (Fig. 1*C*).

RESULTS

Neurons labeled by retrograde transneuronal transport of HSV1 after injections into the arm representation of M1 were found dorsally in the dentate at mid-rostrocaudal levels (Figs. 1, *B* and *C*; 2*B*; and 3*A*). Despite some slight differences in the

injection sites (see Fig. 11 in Hoover and Strick 1999), the three animals with virus injections into the arm area displayed remarkably similar distributions of labeled neurons in the dentate (Figs. 1*C*, 2*B*, and 3*A*). Because of this consistency, we used the origin of input to the arm area of M1 as the "index case" against which the origin of dentate projections to other cortical areas was compared.

In other animals, we placed injections of virus into the leg and face areas of M1 (defined by intracortical stimulation, see Figs. 12 and 13 in Hoover and Strick 1999). Injections into the leg area also labeled neurons in a dorsal portion of the dentate, but in this case at more rostral levels of the nucleus (Fig. 2*A*). Likewise, injections into the face area labeled neurons dorsally in the dentate, but at more caudal levels of the nucleus (Fig. 2*C*). This rostral-to-caudal arrangement of the origin of projections to the leg, arm, and face representations in M1 corresponds well with the somatotopy previously proposed for the dentate (e.g., Allen et al. 1978; Asanuma et al. 1983b; Rispal-Padel et al. 1982; Stanton 1980). In contrast, it should be clear from the unfolded maps that large portions of the dentate nucleus were not labeled following virus injections into M1. As a consequence, the body map generated by the projections to M1 occupied only a portion of the dorsal third of the nucleus.

Some of the dentate regions that were not labeled after virus injections into M1 did contain labeled neurons after injections into prefrontal and posterior parietal areas of the cortex (Clower et al. 2001; Middleton and Strick 2001). For example, virus injections into a part of area 7b located in the intraparietal sulcus resulted in labeled neurons in a ventral portion of caudal dentate (Fig. 3*B*). In contrast, virus injections into a part of area 46 located dorsal to the principal sulcus labeled neurons ventrally at mid rostrocaudal levels of the dentate (Fig. 3*C*). Virus injections into a part of area 9 located on the lateral surface of the hemisphere labeled neurons in yet another part of caudal dentate (Fig. 3*D*). Clearly, a substantial portion of the output from the dentate targets nonmotor areas of cortex in a topo-
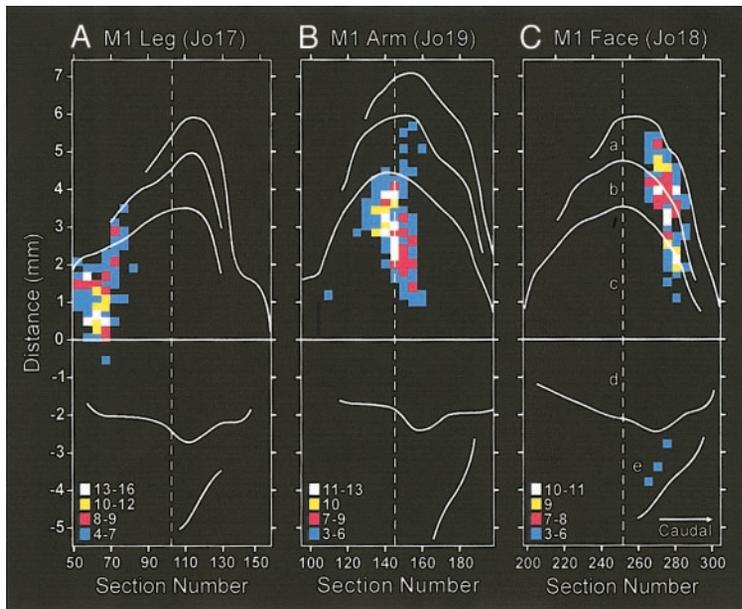
FIG. 2. Somatotopic organization of dentate output channels to M1. Unfolded maps of the dentate illustrate the neurons labeled after HSV1 injections into the *A*: leg, *B*: arm, and *C*: face representations of M1. Conventions and abbreviations as in legend to Fig. 1. The arm case shown in *B* is from a different animal from those illustrated in Figs. 1 and 3*A*.

graphically organized manner (e.g., Clower et al. 2001; Middleton and Strick 1994, 2001).

DISCUSSION

Our results provide new insights into the topographic organization of dentate projections to the cerebral cortex. A summary of our findings is shown on a single unfolded map of the nucleus (Fig. 4*A*). Labels are placed at the sites in the dentate that project most densely to different cortical areas. The origin of projections to the arm representation of the ventral premotor area (PMv) is included in this diagram based on data from Middleton and Strick (1997) (see also Orioli and Strick 1989). This map emphasizes that the dentate is anatomically divided into separate output channels that project to distinct cortical areas.

The unfolded map also illustrates another important perspective about the topographic organization of dentate output–a substantial portion of the nucleus projects to areas of prefrontal and posterior parietal cortex, in addition to its classical motor targets. Furthermore, the output channels that target motor areas of the cortex are segregated from those that target prefrontal and posterior parietal areas of the cortex. Thus the dentate nucleus appears to be functionally divided into separate motor and nonmotor domains.

The motor domain in the dorsal portion of the dentate contains output channels concerned with aspects of movement generation and control. Output neurons that influence leg, arm, and face regions of M1 are arranged in a rostral-to-caudal sequence within the dorsal part of the nucleus (Fig. 4*A*, also see Hoover and Strick 1999). In addition, the motor domain contains distinct output channels that innervate a number of the premotor areas in the frontal lobe (Fig. 4*A*) (Akkal et al. 2001; Dum and Strick 1999; Middleton and Strick 1997). Overall, our current estimate is that the motor domain in the monkey comprises approximately 50–60% of the dentate.
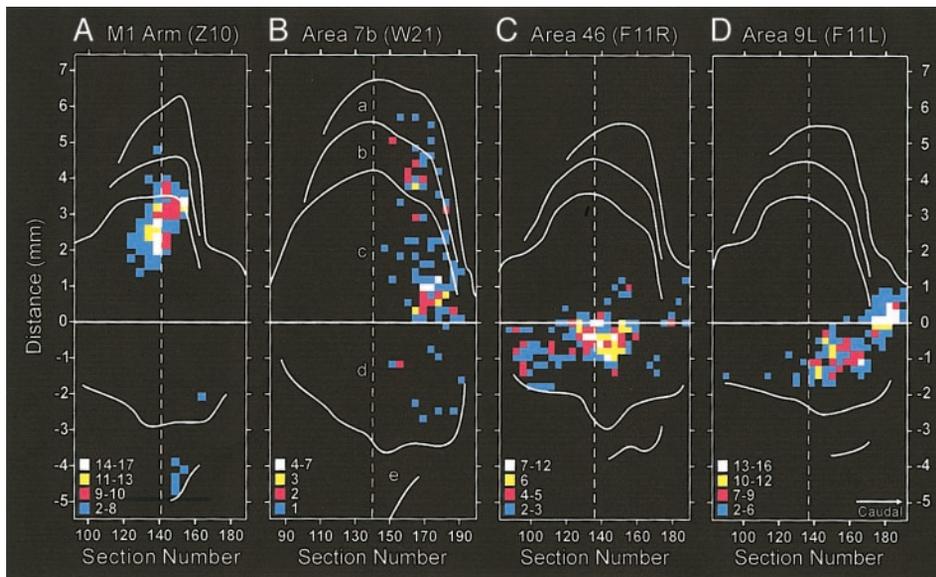
FIG. 3. Dentate output channels to the prefrontal and posterior parietal cortex. Unfolded maps of the dentate illustrate the neurons labeled after HSV1 injections into *A*: arm representation of M1, *B*: area 7b, *C*: area 46, and *D*: area 9l. Conventions and abbreviations as in legend to Fig. 1. The arm case shown in *A* is from a different animal from those illustrated in Figs. 1 and 2*B*.
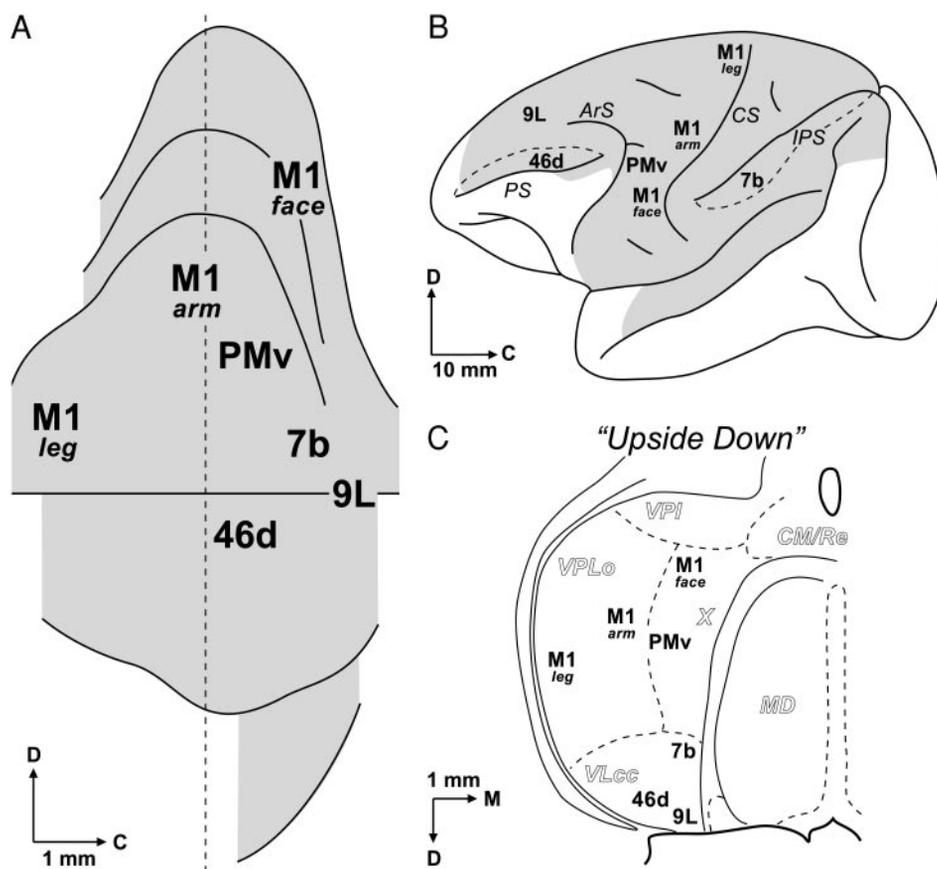
FIG. 4. Topography within the cerebellothalamocortical circuit. *A*: dentate output channels. Origins of the peak density of dentate projections to selected cortical areas are labeled. *B*: selected cortical targets of cerebellothalamocortical circuits. Shading in this diagram indicates the cortical regions (lateral hemisphere only) that project to the cerebellum via the pons (after Brodal 1978; Glickstein et al. 1985; Schmahmann 1998). *C*: origin of selected cortical projections from the ventrolateral thalamus. Cortical regions indicated receive input from regions of the ventrolateral thalamus that lie within the termination zone of cerebellar efferents. The thalamus has been turned upside down to indicate the match between its topography and that of the dentate. ArS, arcuate sulcus; CM/Re, nucleus centrum medianum/nucleus reuniens; CS, central sulcus; IPS, intraparietal sulcus; MD, nucleus medialis dorsalis; PMv- ventral premotor area; PS, principal sulcus; VLcc, caudal portion of the nucleus ventralis lateralis, pars caudalis; VPI, nucleus ventralis posterior inferior; VPLo, nucleus ventralis posterior lateralis, pars oralis; X, area X.

In contrast, the nonmotor domain in the ventral portion of the dentate contains output channels concerned with aspects of cognition and visuospatial function. Within this region, neurons that project to prefrontal and posterior parietal cortical areas are clustered into distinct regions that display little evidence of overlap. Single-neuron recordings in this area have seldom found neurons with changes in activity specifically related to limb movements (e.g., Schieber and Thach 1985; Thach 1978; Wetts et al. 1985). Greater than or equal to 20% of the volume of the dentate is occupied by output channels that innervate portions of areas 9, 46, and 7 (Clower et al. 2001; Middleton and Strick 2001). The cortical targets of the rest of the dentate remain to be determined. However, the amount of the dentate located in the nonmotor domain is likely to grow as projections to other cortical regions are explored.

So far, all the cerebral cortical areas that are the target of dentate output also project back on the cerebellum via efferents to pontine nuclei (i.e., Fig. 4*B*, shaded region) (Brodal 1978; Glickstein et al. 1985; Schmahmann 1998). Conversely, cortical areas that do not project back on the cerebellum do not appear to be the target of dentate output (e.g., the ventral portion of area 46, the lateral portion of area 12, and area TE

in inferotemporal cortex) (for discussion see Middleton and Strick 1996, 2001). These observations lead to the conclusion that multiple closed-loop circuits appear to be a major functional unit of cerebrocerebellar circuitry (Middleton and Strick 1998). This arrangement suggests that some of the unknown targets of dentate output are other nonmotor areas that are known to provide input to the cerebellum (e.g., portions of area 5, area 7, and anterior and posterior cingulate cortex) (Brodal 1978; Glickstein et al. 1985; Schmahmann 1998). We are currently testing this prediction.

Molecular markers may also prove useful for identifying the full extent of the nonmotor domain of the dentate. Immunostaining with 8B3, an antibody that recognizes a novel proteoglycan epitope localized on cell membranes, stains ventral regions of the macaque dentate more intensely than more dorsal regions (Pimenta et al. 2001). Similarly, immunostaining for two calcium-binding proteins, calretinin and parvalbumin, is reported to be greatest in ventral regions of the squirrel monkey dentate (Fortin et al. 1998). The precise correlation between these differential patterns of immunostaining and the functional topography of the dentate remains to be determined. However, if a match exists, these molecular markers may provide a bridge for constructing homologies between the

motor and nonmotor domains in the monkey and human dentate.

Mapping of dentate output channels onto the thalamus

To understand how the output of the dentate maps on the ventrolateral thalamus, we have displayed the origin of efferents to different cortical areas on a single section through the thalamus (Fig. 4*C*). Labels are placed at sites in the ventrolateral thalamus that receive cerebellar efferents and project to the cortical areas indicated. Although this map is a considerable simplification of the complex three-dimensional architecture of thalamocortical relationships, it has some important heuristic value. For example, the *rostral to caudal* topography in the dentate appears to translate into a *lateral to medial* topography in the thalamus. Within the motor domain of the dentate, the *rostral-leg to caudal-face* somatotopy (Fig. 4*A*) is transformed into a *lateral-leg to medial-face* somatotopy in the ventrolateral thalamus (Fig. 4*C*) (Kievit and Kuypers 1977; Miyata and Sasaki 1983; Strick 1976a,b; Vitek et al. 1994). A similar topographic mapping appears to be present between the output channels in the ventral, nonmotor domain of the dentate and VLcc in the thalamus.

A comparison of the dentate and thalamic maps also illustrates that the *dorsal to ventral* topography in the dentate is inverted to form a *ventral to dorsal* topography in the thalamus. As a consequence, we have portrayed the thalamus *upside down* to maintain the correspondences between the maps (compare Fig. 4, *A* with *C*). The motor and nonmotor domains of the dentate project to distinct territories in the ventrolateral thalamus (Fig. 4, *A* and *C*). Efferents from the dorsal, motor domain of the dentate project on the classic motor subdivisions of the ventrolateral thalamus (e.g., VPLo and area X according to Olszewski 1952). In contrast, efferents from the ventral, nonmotor domain terminate more dorsally in portions of VLcc (Fig. 4*C*) (VLcc according to Holsapple et al. 1991). Thus, in both the dentate and VLcc, projections to widely dispersed areas of prefrontal and posterior parietal cortex have been collected together.

The dominant view of the cerebellum over the last century has been that it is concerned with the coordination and control of motor activity (Brooks and Thach 1981). It is now clear that the anatomical substrate exists for cerebellar output to influence nonmotor as well as motor areas of the cerebral cortex (Clower et al. 2001; Hoover and Strick 1999; Middleton and Strick 1998, 2001). Our map shows that a significant portion of the output from the cerebellum is directed to cortical regions thought to be involved in cognitive and visuospatial functions (Clower et al. 2001; Middleton and Strick 2001). Indeed, ventral portions of dentate are activated during a variety of tasks involving short-term working memory, rule-based learning, and higher executive function–like planning (Kim et al. 1994; Jueptner et al. 1997; Liu et al. 2000; Mushiake and Strick 1993). There is evidence that the proportion of dentate output to cortical regions involved in cognitive functions is larger in humans than monkeys (Leiner et al. 1991; Matano 2001). Thus the dentate's participation in nonmotor functions may be expanded in the human (e.g., Schmahmann and Sherman 1998).

Our results along with recent physiological observations (Kim et al. 1994; Jueptner et al. 1997; Liu et al. 2000; Mushiake and Strick 1993) suggest that there is a topography of

function within the dentate. The nucleus clearly contains separate motor and nonmotor domains. Our unfolded map of the nucleus, like other flattened maps, provides a consistent anatomical framework for future explorations into the topography of function in the dentate.

REFERENCES

Akkal D, Dum RP, and Strick PL. Cerebellar and pallidal inputs to the supplementary motor area (SMA). *Soc Neurosci Abstr* 27: 825.4, 2001.

Allen GI, Gilbert PF, and Yin TC. Convergence of cerebral inputs onto dentate neurons in monkey. *Exp Brain Res* 32: 151–170, 1978.

Asanuma C, Thach WT, and Jones EG. Distribution of cerebellar terminations and their relation to other afferent terminations in the ventral lateral thalamic region of the monkey. *Brain Res Rev* 5: 237–265, 1983a.

Asanuma C, Thach WT, and Jones EG. Anatomical evidence for segregated focal groupings of efferent cells and their terminal ramifications in the cerebellothalamic pathway of the monkey. *Brain Res Rev* 5: 267–297, 1983b.

Brodal A. Experimentelle Untersuchungen über die olivocerebellare Lokalisation. *Z Gesamte Neurol Psychiat* 169: 1–153, 1940.

Brodal P. The corticopontine projection in the rhesus monkey: origin and principles of organization. *Brain* 101: 251–283, 1978.

Brooks VB and Thach WT. Cerebellar control of posture and movement. In: *Handbook of Physiology. The Nervous System. Motor Control.* Bethesda, MD: Am. Physiol. Soc, 1981, sect. 1, vol. II, p. 877–946.

Clower DM, West RA, Lynch JC, and Strick PL. The inferior parietal lobule is the target of output from the superior colliculus, hippocampus and cerebellum. *J Neurosci* 21: 6283–6291, 2001.

Dum RP and Strick PL. The origin of corticospinal projections from the premotor areas in the frontal lobe. *J Neurosci* 11: 667–689, 1991.

Dum RP and Strick PL. Pallidal and cerebellar inputs to the digit representations of the dorsal and ventral premotor areas (PMd and PMv). *Soc Neurosci Abstr* 25: 1925, 1999.

Fiez JA, Petersen SE, Cheney MK, and Raichle ME. Impaired non-motor learning and error detection associated with cerebellar damage: a single case study. *Brain* 115: 155–178, 1992.

Fortin M, Marchand R, and Parent A. Calcium-binding proteins in primate cerebellum. *Neurosci Res* 30: 155–168, 1998.

Glickstein M, May III JG, and Mercier BE. Corticopontine projection in the macaque: the distribution of labeled cortical cells after large injections of horseradish peroxidase in the pontine nuclei. *J Comp Neurol* 235: 343–359, 1985.

He SQ, Dum RP, and Strick PL. Topographic organization of corticospinal projections from the frontal lobe: motor areas on the medial surface of the hemisphere. *J Neurosci* 15: 3284–3306, 1995.

Holsapple JW, Preston JB, and Strick PL. The origin of thalamic inputs to the 'hand' representation in the primary motor cortex. *J Neurosci* 11: 2644–2654, 1991.

Hoover JE and Strick PL. The organization of cerebellar and basal ganglia outputs to primary motor cortex as revealed by retrograde transneuronal transport of herpes simplex virus type 1. *J Neurosci* 19: 1446–1463, 1999.

Ivry RB, Keele SW, and Diener HC. Dissociation of the lateral and medial cerebellum in movement timing and movement execution. *Exp Brain Res* 73: 167–180, 1988.

Jueptner M, Frith CD, Brooks DJ, Frackowiak RSJ, and Passingham RE. Anatomy of motor learning. II. Subcortical structures and learning by trial and error. *J Neurophysiol* 77: 1325–1337, 1997.

Kemp JM and Powell TPS. The connexions of the striatum and globus pallidus: synthesis and speculation. *Philos Trans R Soc Lond B* 262: 441–457, 1971.

Kievit J and Kuypers HG. Organization of the thalamo-cortical connexions to the frontal lobe in the rhesus monkey. *Exp Brain Res* 29: 299–322, 1977.

Kim S-G, Ugurbil K, and Strick PL. Activation of cerebellar output nucleus during cognitive processing. *Science* 265: 949–951, 1994.

Larsell O. *The Comparative Anatomy and Histology of the Cerebellum from Monotremes Through Apes.* Minneapolis, MN: The University of Minnesota Press, 1970.

Leiner HC, Leiner AL, and Dow RS. The human cerebro-cerebellar system: its computing, cognitive, and language skills. *Behav Brain Res* 44: 113–128, 1991.

Liu Y, Pu Y, Gao JH, Parsons LM, Xiong J, Liotti M, Bower JM, and Fox PT. The human red nucleus and lateral cerebellum in supporting roles for sensory information processing. *Hum Brain Mapping* 10: 147–159, 2000.

Lynch JC, Hoover JE, and Strick PL. Input to the primate frontal eye field from the substantia nigra, superior colliculus, and dentate nucleus demonstrated by transneuronal transport. *Exp Brain Res* 100: 181–186, 1994.

Matano S. Brief communication: proportions of the ventral half of the cerebellar dentate nucleus in humans and great apes. *Am J Phys Anthropol* 114: 163–165, 2001.

Middleton FA and Strick PL. Anatomical evidence for cerebellar and basal ganglia involvement in higher cognitive function. *Science* 266: 458–461, 1994.

Middleton FA and Strick PL. New concepts regarding the organization of basal ganglia and cerebellar output. In: *Integrative and Molecular Approach to Brain Function*, edited by M. Ito and Y. Miyashita. Amsterdam: Elsevier Science, 1996, p. 253–269.

Middleton FA and Strick PL. Dentate output channels: motor and cognitive components. In *Progress in Brain Research. The Cerebellum from Structure to Control*, edited by C. I. De Zeeuw, P. Strata, and J. Voogd. Amsterdam: Elsevier, 1997, vol. 114, p. 553–566.

Middleton FA and Strick PL. Cerebellar output: motor and cognitive channels. *Trends Cogn Sci* 2: 348–354, 1998.

Middleton FA and Strick PL. Cerebellar 'projections' to the prefrontal cortex of the primate. *J Neurosci* 21: 700–712, 2001.

Miyata M and Sasaki K. HRP studies on thalamocortical neurons related to the cerebellocerebral projection in the monkey. *Brain Res* 274: 213–224, 1983.

Mushiake H and Strick PL. Preferential activity of dentate neurons during limb movements guided by vision. *J Neurophysiol* 70: 2660–2664, 1993.

Olszewski J. *The Thalamus of the Macaca mulatta: An Atlas for use with the Stereotaxic Instrument.* Basel: Karger, 1952.

Orioli PJ and Strick PL. Cerebellar connections with the motor cortex and the arcuate premotor area: an analysis employing retrograde transneuronal transport of WGA-HRP. *J Comp Neurol* 288: 612–626, 1989.

Pimenta AF, Strick PL, and Levitt PR. A novel proteoglycan epitope is expressed in functionally discrete patterns in primate cortical and subcortical regions. *J Comp Neurol* 430: 369–388, 2001.

Ramnani N and Miall C. Expanding cerebellar horizons. *Trends Cogn Sci* 5: 135–136, 2001.

Rispal-Padel L, Cicirata F, and Pons C. Cerebellar nuclear topography of simple and synergistic movements in the alert baboon (*Papio papio*). *Exp Brain Res* 47: 365–380, 1982.

Schieber MH and Thach WT. Trained slow tracking. II. Bidirectional discharge patterns of cerebellar nuclear, motor cortex and spindle afferent neurons. *J Neurophysiol* 54: 1228–1270, 1985.

Schmahmann JD. *The Cerebellum and Cognition. International Review of Neurobiology*, edited by J. D. Schmahmann. San Diego: Academic Press, 1997, vol. 41.

Schmahmann JD. Dysmetria of thought: clinical consequences of cerebellar dysfunction on cognition and affect. *Trends Cogn Sci* 2: 362–371, 1998.

Schmahmann JD and Sherman JC. The cerebellar cognitive affective syndrome. *Brain* 121: 561–579, 1998.

Special Issue. The cerebellum: development, physiology and plasticity. *Trends Neurosci* 21: 376–418, 1998.

Special Issue. The cerebellum: connections, computations and cognition. *Trends Cogn Sci* 2: 305–371, 1998.

Stanton GB. Topographical organization of ascending cerebellar projections from the dentate and interposed nuclei in *Macaca mulatta*: an anterograde degeneration study. *J Comp Neurol* 190: 699–731, 1980.

Strick PL. Anatomical analysis of ventrolateral thalamic input to the primate motor cortex arm area. *J Neurophysiol* 39: 1020–1031, 1976a.

Strick PL. Activity of ventrolateral thalamic neurons during movement. *J Neurophysiol* 39: 1032–1044, 1976b.

Strick PL and Card JP. Transneuronal mapping of neural circuits with alpha herpes viruses. In: *Experimental Neuroanatomy: a Practical Approach*, edited by J. P. Bolam. Oxford: Oxford University Press, 1992, p. 81–101.

Thach WT. Correlation of neural discharge with pattern and force of muscular activity, joint position, and direction of intended next movement in motor cortex and cerebellum. *J Neurophysiol* 41: 654–676, 1978.

Van Essen DC and Drury HA. Structural and functional analyses of human cerebral cortex using a surface-based atlas. *J Neurosci* 17: 7079–7102, 1997.

Van Essen DC and Maunsell JH. Two-dimensional maps of the cerebral cortex. *J Comp Neurol* 191: 255–281, 1980.

Van Essen DC, Lewis JW, Drury HA, Hadjikhani N, Tootell RB, Bakircioglu M, and Miller MI. Mapping visual cortex in monkeys and humans using surface-based atlases. *Vision Res* 41: 1359–1378, 2001.

Vitek JL, Ashe J, DeLong MR, and Alexander GE. Physiologic properties and somatotopic organization of the primate motor thalamus. *J Neurophysiol* 71: 1498–1513, 1994.

Wetts R, Kalaska JF, and Smith AM. Cerebellar nuclear cell activity during antagonist cocontraction and reciprocal inhibition of forearm muscles. *J Neurophysiol* 54: 231–244, 1985.